Journal of Thermal Analysis and Calorimetry, Vol. 92 (2008) 2, 443–449

STRUCTURAL PROPERTY AND FUNCTION OF *D-ERYTHRO* ASYMMETRIC CHAIN SPHINGOMYELINS AS STUDIED BY MICROCALORIMETRY AND ELECTRON MICROSCOPY

*H. Aoki, S. Kosakabe, M. Inumaru, A. Kuboki, S. Ohira and M. Kodama**

Department of Biochemistry, Faculty of Science, Okayama University of Science, 1-1 Ridai-cho, Okayama 700-0005, Japan

D-erythro sphingomyelines (SM) having a defined acyl chain were synthesized with sphingosylphosphorylcholine as a starting material, and both a structural property and its relating phase transition phenomenon were compared between a symmetric chain length SM (palmitoyl-SM: C16-SM) and asymmetric chain length SMs (behenoyl-SM: C22-SM, lignoceryl-SM: C24-SM). Furthermore, effect of increasing a content of asymmetric chain SMs in the mixture systems of C22-SM/C16-SM, and C24-SM/C16-SM was investigated.

The present calorimetric and electron microscopic studies revealed that (1) The main transition enthalpy is smaller for the asymmetric chain SMs than for the symmetric chain SM by about 3 kJ mol^{-1}, although the acyl chain length is longer for the former than for latter; (2) Relatively small size vesicles (100~200 nm diameters) surrounded by one or more lamellae are observed for the asymmetric chain SMs, in contrast to large multilamellar vesicles (1500~2500 nm diameters) having at least fifteen stained lamellae for the symmetric chain SM and (3) The coexisting asymmetric chain SMs cause the decrease in size and multiplicity for the MLV of the symmetric chain SM, simultaneously with a decrease in the main transition enthalpy.

Keywords: *DSC, D-erythro symmetric and asymmetric chain sphingomyelins, geometric packing shape, negative stain electron microscopy*

Introduction

In 1997, lipid microdomains, generally known as rafts and caveolae, have been reported to be formed within cell membranes and also a large portion of sphingolipids has been found to localize in the microdomains [1–4]. The sphingolipids are clearly distinguished from glycerolipids on the basis of the difference in a backbone structure, thus, a sphingosine for the former and a glycerol for the latter [5–18]. From this viewpoint, structural and functional properties of the sphingolipids in biomembranes have been the subject of many investigations. In these past studies [5–11], a sphyngomyelin (SM) having a phosphorylcholine headgroup has been the most frequently taken up and it has been reported that naturally occurring SM is present in various molecular species of different acyl chain lengths ranging from 14 to 24 carbons, in contrast to a fixed chain length (mostly 18 carbons long) for the other sphingosine chain. In this connection, studies on the intramolecular chain length asymmetry of SMs have been recognized as the subject of investigations [19]. However, there is a problem that the asymmetric chain SMs having a defined acyl chain are commercially unavailable. So, a synthesis by workers themselves is required to obtain the acyl chain-defined SMs, and a semisynthesis due to a deacylation – reacylation of the natural SM has been used in many past studies of this area [9–13], but the semisynthesis has been revealed to accompany an epimerization of *D-erythro* to L-*threo* configurations in the deacylation process.

The present study aims to make clear the structural property of *D-erythro* asymmetric chain SMs in comparison with a *D-erythro* symmetric chain SM. These SMs were synthesized by an acylation of commercially available *D-erythro*-sphingosylphosphocholine (SPC) [6, 10]. Thermotropic behavior of these SM dispersions was investigated by a high-sensitivity differential scanning calorimetry (DSC) and their vesicular structure was examined by a negative stain electron microscopy.

Experimental

Materials

D-erythro-sphingosylphosphorylcholine (SPC) (Lot No.: SPHPC-16) was purchased from Avanti polar lipids, Inc. (Birmingham, AL). The purity >99% for the *D-erythro*-SPC was checked by a combination of high performance liquid chromatography and positive ion electrospray ionization mass spectroscopy (ESI/MS), and the *D-erythro*-SPC was used without

* Author for correspondence: kodama@dbc.ous.ac.jp

1388–6150/$20.00

Akadémiai Kiadó, Budapest, Hungary
Springer, Dordrecht, The Netherlands

further purification. Fatty acids such as palmitic acid (C16:0), behenic acid (C22:0), and lignoceric acid (C24:0) were purchased from Tokyo Kasei kogyo Co., Ltd. (Tokyo, Japan). Cyclohexylamine and dicyclohexylcarbodiimide were obtained from Fluka (Buchs, Switzerland).

Synthesis, purification, and identification of *D-erythro*-sphingomyelins

Synthesis: *D-erythro*-2-*N*-palmitoylsphingosyl-1-phosphocholine (C16-SM), *D-erythro*-2-*N*-behenoylsphingosyl-1-phosphocholine (C22-SM), and *D-erythro*-2-*N*-lignocerylsphingosyl-1-phosphocholine (C24-SM) were synthesized from *D-erythro*-SPC and respective fatty acids essentially according to a DCC method previously reported by Cohen *et al.* [6] and Ramsteadt *et al.* [11]. For example, the synthesis of *D-erythro*-C16-SM having an acyl chain of 16 carbons long is as follows: the SPC (27 mg) and a large molar excess of palmitic acid (83 mg, 5.7 mol/mol SPC) were dissolved with stirring in a mixture of solvents (3.3 mL of dichloromethane plus 0.3 mL of methanol) containing ~20 grains of Molecular Sieves 4A, and both dicyclohexylcarbodiimide in a large molar excess with respect to the fatty acid (3.4:1.0 mol/mol) and cyclohexylamine in a slight molar excess with respect to the SPC(6.0:5.7 mol/mol) were added. A temperature of the reaction mixture was raised to 40°C, at which constant stirring was continued for at least 20 h. The disappearance of SPC and the formation of C16-SM were monitored by thin layer chromatography (TLC) on silica gel G plates, developed with chloroform/ methanol/concentrated ammonia/water (65:35:2.5:2.5 vol) [6]. The reaction mixture was filtered to remove the molecular sieve. The solvents were removed on a rotary evaporator under reduced pressure.

Purification: the C16-SM thus obtained was purified by silica gel column chromatography (Silica Gel 60, 70–230 mesh in size) using gradient elution with methanol/ chloroform ranging in volume ratio from 9:1 to 1:1. The purification was continued until no change in the half-height width of the gel-to-liquid crystal phase transition peak was observed by DSC and no peak due to impurities was detected by the mass spectrometry.

Identification: the identification of the purified C16-SM was performed with ^{13}C- and ^{1}H-NMR, high performance TLC (HPTLC), and electrospray ionization mass spectrometry (ESI/MS). The chemical shifts for both carbons of C-5, C-4 and C-3 and protons of 3-H and 2-H of the sphingosine backbone were obtained with JNM-GSX400 spectrometer at 400 MHz and were compared with results previously reported by Bruzik [20]. The molecular configuration at C-3 position of the sphingosine of the synthesized SM was confirmed to be *D-erythro* form, indicating no existence of L-*threo* SM. The validity of the result was ascertained by high performance TLC (HPTLC) using chloroform/methanol/water (25:10:1.1 vol) [21, 22] and a single-band pattern was observed, showing no occurrence of epimerization in the synthesis procedure [22]. The molecular mass of the SM was determined with JMS-LCmate electrospray ionization mass spectrometer (JEOL, Japan) detecting positive ESI spectrum found as $[SM+Na]^+$ [23] and the resulting molecular mass matched the expected value.

Asymmetric chain length SMs, C22-SM and C24-SM, were synthesized by the procedure described above and both the purification and identification of these SMs were the same as those described above.

Preparation of vesicle dispersions

Vesicle dispersions of respective synthesized *D-erythro* SMs were prepared according to a Bangham method [12]: a lipid film was first prepared by removing chloroform from the lipid stock solution on a rotary evaporator, and then under high vacuum (10^{-4} Pa) to achieve complete removal of traces of the solvent. The dried lipid film thus obtained was suspended in distilled water, and gently vortexed at a desired temperature above the gel-to-liquid crystal phase transition (main transition).

A study on the structural function of the asymmetric chain length SMs, C22-SM and C24-SM, for the symmetric chain length C16-SM was performed with vesicle dispersions prepared from a mixed film of two lipids. For example, the film used to prepare the dispersion of C24-SM/C16-SM system was formed by adding desired amounts of the C24-SM stock solution to the C16-SM stock solution and then removing chloroform solvent. In this experiment, the lipid concentrations of the individual stock solutions were previously determined by a modified Bartlett phosphate assay [13] before mixing, and a content of the C24-SM in the mixed film was varied from 5 to 100 mol%. The resulting vesicle dispersions were annealed by repeating thermal cycling at temperatures above and below the main transition to attain homogenous mixing of the two lipids and the annealing was continued until no changes in thermal behavior were observed by DSC. The same method was applied to prepare the C22-SM/C16-SM vesicle dispersions at varying C22-SM content.

Methods

Differential scanning calorimetry (DSC): all calorimetric experiments were performed with a VP differential scanning microcalorimeter (Microcal Inc., Northampton, MA) characterized by a short-term noise of 4.184 μJ min^{-1} (=0.07 μW) and on heating from 0°C

to temperatures of the liquid crystal phase at a rate of 45°C h^{-1}. The lipid concentrations in the present DSC experiments were ~0.5 mM with a calorimetric cell volume of 0.52 mL. After the DSC, the lipid concentrations were determined by a modified Bartlett phosphate assay [13]. Accordingly, for the C22-SM/C16-SM, and C24-SM/C16-SM systems, the total lipid concentration involving the two lipids was estimated, and so the molar transition enthalpies of these systems are given in mol of whole lipids.

Negative stain electron microscopy: the vesicular structure of the gel phase was examined with electron microscopes of a JEOL JEM-2000EX and a Hitachi H-8100. All preparations used for the electron microscopy were prepared at room temperature as follows [14]: a drop of vesicle dispersions (lipid concentration: ~1 mM) was placed on copper grids covered with carbon-coated collodion films, allowed to remain until becoming dry, after which a drop of 2% solution of sodium phosphotungstate (pH approximately 7) used as a stainer was added and the excess solution was then drained. All the preparations were supplied immediately to the electron microscopy operated at around 20°C.

Results and discussion

DSC: Vesicle dispersions of the purified D-*erythro* C16-SM, C22-SM and C24-SM were transferred into the calorimetric cell at 0°C and heating scans performed immediately on cooling after a heating scan were repeated until no change in transition behavior was observed. In Fig. 1, the resultant limiting transition behavior, which is reversible and reproducible, is compared for the C16-SM (Fig. 1a), C22-SM (Fig. 1b) and C24-SM vesicle dispersions (Fig. 1c). The three SMs show two transitions of minor and major observed in low- and high-temperature sides, respectively. The miner transition for the C16-SM (Fig. 1a) has been reported to be comparable to the gel ($L_{\beta'}$)-to-gel ($P_{\beta'}$) phase transition, generally called the pretransition [9], which is subsequently followed by the gel ($P_{\beta'}$)-to-liquid crystal phase transition, generally called the main transition. Similarly, the miner and major transitions for the C22-SM (Fig. 1b) could be assigned to the pretransition and the main transition, respectively. However, the enthalpy change of the miner transition of the C24-SM (Fig. 1c) is much larger, and so the transition cannot be accounted well for by the pretransition alone [7]. Therefore, it seems reasonable to assume that the transition under consideration accompanies a change of packing arrangements of the C24-SM in an intrabilayer [9, 24], so that the transition is designated as the gel-to-gel phase transition in the present study. As shown in Fig. 1a, the C16-SM shows a cooperative

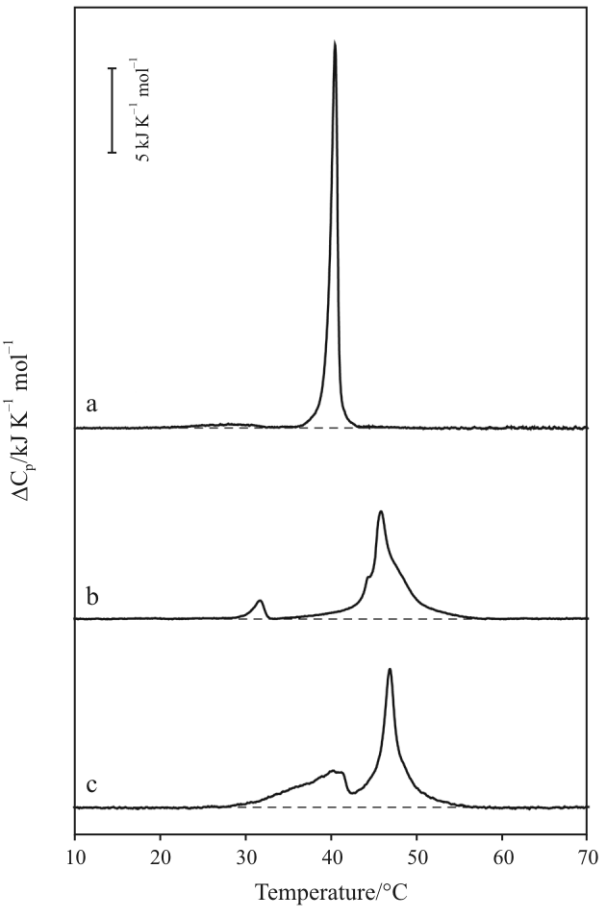

Fig. 1 Limiting phase transition behavior in a heating scan obtained after repeating thermal cyclings at temperatures of 0 to 70°C for vesicle dispersions of the synthesized *D-erythro* a – C16-SM, b – C22-SM and c – C24-SM. Apparent excess heat capacity (ΔC_p) is plotted as a function of temperature (t)

sharp main transition at 40.4°C with a large transition enthalpy (ΔH=33.5 kJ mol^{-1}) [9, 22]. However, in Fig. 1b for the C22-SM, a complex main transition (ΔH=30.5 kJ mol^{-1}) is observed with a peak maximum at 45.8°C, simultaneously with both a poorly resolved shoulder on the high temperature side and a resolved shoulder on the low temperature side. The C24-SM (Fig. 1c) also shows a complex main transition (ΔH=30.1 kJ mol^{-1}) with a peak maximum at 46.7°C and two poorly resolved shoulders which appear on the low and high temperature sides, respectively.

Table 1 summarizes thermal data associated with the phase transitions of three *D-erythro* SMs. In this table, the transition temperatures are represented by the maximum in the ΔC_P *vs. t* curves shown in Fig. 1. For the C24-SM, a deconvolution analysis performed with a computer program (ORIGIN, Microcal Software Inc., Northampton, MA) was used to obtain the gel-to-gel phase transition and main transition enthalpies, since two transition peaks overlap at their

bases (Fig. 1c) [16]. The main transition enthalpies of the asymmetric chain SMs are smaller than that of the symmetric chain SM although the acyl chain length of the former is longer than that of the latter. In this respect, we call attention to a much smaller main transition enthalpy (ΔH=18.8 kJ mol^{-1}) reported by Bar *et al.* [9] for the synthesized *D-erythro* C24-SM and nearly the same main transition enthalpy (ΔH=35.1 kJ mol^{-1}) reported by Ramstedt *et al.* [22] for the synthesized *D-erythro* C16-SM although comparable thermal data are scarce for *D-erythro* SMs.

Figure 2 shows thermal behavior of the C22-SM/C16-SM (Fig. 2A) and C24-SM/C16-SM systems (Fig. 2B), for which contents of the individual asymmetric chain SMs are 0, 5, 30, 50, 75 and 100 mol%. In Fig. 2, it is clear that the sharp main transition of the C16-SM becomes broader with increasing a content of the asymmetric chain SMs. In Fig. 3, the main transition enthalpies per mole of whole lipids for two systems are plotted against the content of the respective asymmetric chain SMs. The main transition enthalpies of the C22-SM/C16-SM (Fig. 3a) and C24-SM/C16-SM systems (Fig. 3b) gradually decrease with increasing a content of the asymmetric chain SMs, and finally to respective limiting values corresponding to the main transition enthalpies of the C22-SM and C24-SM.

Table 1 Thermal data associated with phase transitions of the synthesized *D-erythro* C16-, C22- and C24-SMs. The transition temperatures T_m refer to the maximum in the ΔC_p *vs. t* curves and ΔH is the enthalpy change associated with the phase transitions shown in Fig. 1

	Gel-to-gel phase transition		Main transition	
	T_m/ °C	ΔH/ kJ mol^{-1}	T_m/ °C	ΔH/ kJ mol^{-1}
C16-SM	27.5	0.7	40.4	33.5
C22-SM	31.7	2.2	45.8	30.5
C24-SM	40.0	18.1	46.7	30.1

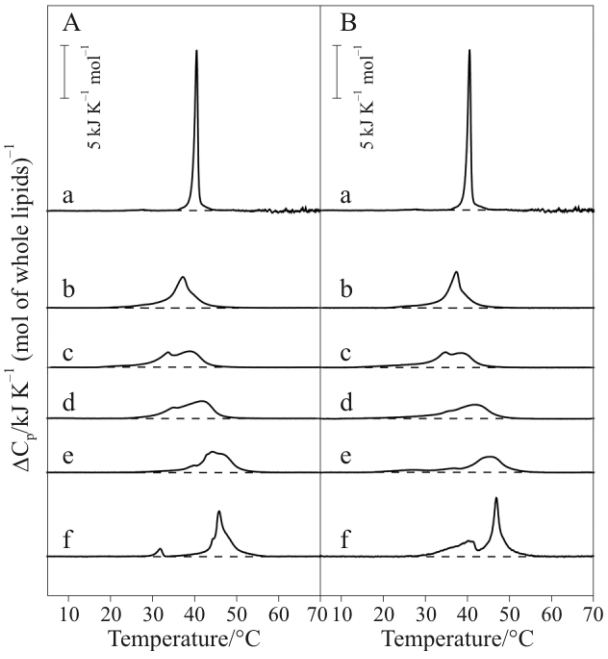

Fig. 2 Phase transition behavior for vesicle dispersions of the synthesized *D-erythro* A – C22-SM/C16-SM and B – C24-SM/C16-SM systems. Contents of C22-SM and C24-SM (mol%): a – 0, b – 5, c – 30, d – 50, e – 75, f – 100. Apparent excess heat capacity (ΔC_p) is given in mol of whole lipids

Electron microscopy: the vesicular structure of the low temperature gel phase was examined for the three *D-erythro* SMs with a negative stain electron microscopy. In Fig. 4, the typical micrograph is compared for the C16-SM (Fig. 4a), C22-SM (Fig. 4b), and C24-SM (Fig. 4c). The symmetric chain C16-SM shows large multilamellar vesicles (MLVs) of mean diameter ~2 μm, which is in accord with a result obtained by Bar *et al.* [9]. Also, such a micrographic profile has been reported for symmetric chain diacylphosphatidylcholines (DMPC, DPPC) [14]. However, profiles of the asymmetric chain SMs are quite different. Thus, as shown in Fig. 4b, for the C22-SM, relatively small size vesicles of ~200 nm in mean diameter are observed to have a well-defined internal cavity surrounded by a few lamellae and their size is approximately 10 times smaller that of the MLVs of the symmetric chain C16-SM (Fig. 4a). As shown in Fig. 4c, the decrease in both size and multiplicity in comparison with the MLVs is more pronounced for the C24-SM: the highly asymmetric chain SM presents only unilamellar vesicles of ~100 nm in mean diameter. The similar unilamellar

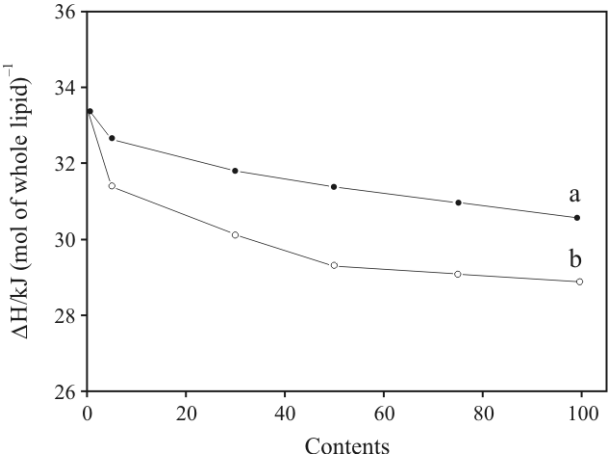

Fig. 3 Effect of increasing a content of the asymmetric C22- and C24-SMs on the main transition enthalpy of a – C22-SM/C16-SM and b – C24-SM/C16-SM systems

vesicles, although smaller in size (~75 nm in diameter), have been reported for the synthesized *D-erythro* C24-SM by Bar *et al.* [9]. The micrographic results demonstrate that a characteristic feature of the asymmetric chain SMs in aqueous medium is their ability to form relatively small size vesicles having an internal water pool surrounded by one or more lamellae.

Figure 5 shows representative micrographs obtained for the C24-SM/C16-SM mixture system at the C24-SM contents of 5 (Fig. 5a) and 50 mol% (Fig. 5b). When compared with the MLV of the C16-SM vesicle shown in Fig. 4a, it is obvious that the presence of the C24-SM, even at a content of as low as 5 mol% (Fig. 5a), causes drastic decreases in size and multiplicity of the vesicle. Such a structural change proceeds more and more with increasing the content of C24-SM, giving rise to mostly unilamellae vesicles of 150~200 nm diameters observed at 50 mol% of C24-SM (Fig. 5b).

The following results were obtained by the present calorimetric and electron microscopic studies:

1. The main transition enthalpy is smaller for the asymmetric chain C22- and C24-SMs than for the symmetric chain C16-SM by about 3 kJ/mol, although the acyl chain length is longer for the former than for the latter (Table 1).

2. Relatively small size vesicles (100~200 nm diameters) surrounded by one or more lamellae are observed for the asymmetric chain SMs, in contrast to large multilamellar vesicles (1500~2500 nm diameters) having at least fifteen stained lamellae (Fig. 4).

3. The coexisting asymmetric chain SMs cause the decrease in size and multiplicity for the MLV of the symmetric chain SM (Fig. 5), simultaneously with a decrease in the main transition enthalpy (Fig. 3).

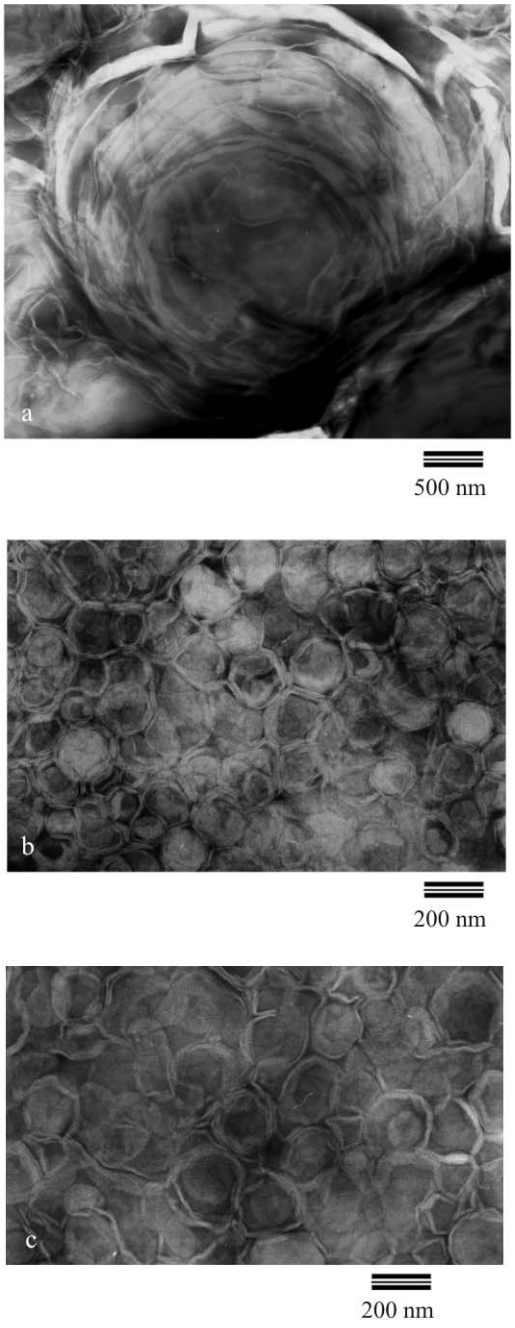

Fig. 4 Electron micrographs of the synthesized *D-erythro* sphingomyelins: a – C16-SM; b – C22-SM and c – C24-SM

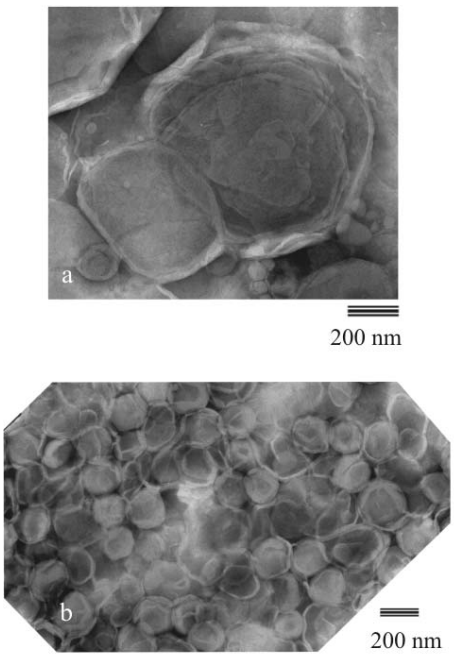

Fig. 5 Electron micrographs of the C24-SM/C16-SM system at different contents of the C24-SM (mol%): a – 5 and b – 50

From the viewpoint of geometric packing shape of lipid molecules in a vesicle bilayer, we discuss why the asymmetric chain SMs are possible to form the small size vesicles observed in the present study. Such small size vesicles are characterized by the limiting phase transitions observed after repeated heating scans. When the dispersion of C24-SM was prepared at temperatures as low as ~10°C and was then transferred into the calorimetric cell at 0°C, 1.5 times increment of the low temperature transition (gel-to-gel phase transition) enthalpy was observed (not shown data), suggesting a polymorphism for the asymmetric chain SM (results of the polymorphism will be detailed in the following paper). On this basis, it is considered that the small size vesicles observed in the low temperature gel phase for the asymmetric chain SM are metastable, but their stability is fairly high. This is because no changes in both the vesicular form and the phase transition behavior were observed, even when the dispersion of the asymmetric chain SM was stored at 5°C for three months. By reference to a paper reported by Huang *et al.* [25], it is noted that small unilamellar vesicles (SUVs) are attained only when a higher degree of surface curvature of the inner monolayer relative to the outer monolayer is realized in the vesicle bilayer. This requires a lipid molecule in the inner monolayer to adopt a truncated cone packing shape, for which the effective surface area occupied by two chains is larger than that for a polar headgroup. Accordingly, it is almost certain that the asymmetric chain C24-SM molecule in the inner monolayer adopts more or less the truncated cone shape although the vesicle size of the asymmetric chain SM is not so small as that (<50 nm) of the so-called SUV. Here, we refer to the model conformation of the C24-SM molecule (Fig. 6) constructed on the basis of PDB file [26] which is essentially the same as that reported Huang and Mason [27]. It can be seen that in the intramolecule the acyl chain is 10.5 C–C bond lengths (11.5 carbon atoms) longer than the sphingosine chain. A generally accepted packing arrangement for the C24-SM is a partial interdigitation [7, 8], i.e., the short sphingosine chain of the SM molecule in a monolayer packs end-to-end with the long acyl chain of another SM molecule present in the opposing bilayer monolayer. For this partial interdigitation, we focus on disordering effects of a terminal bulky methyl end which exerts, even in the solid-state of gel phase, on neighboring hydrocarbon chains [28]. Thus, on this basis, the terminal methyl group of the short sphingosine chain is considered to induce conformational changes such as trans→ gauche isomerizations for extra 10.5 C–C bonds of the acyl chain. Such conformational changes would cause

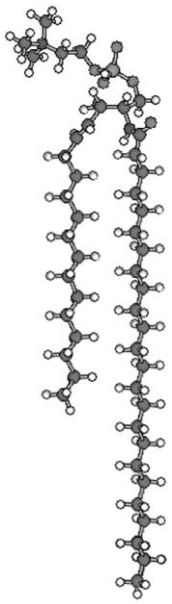

Fig. 6 Model conformation of *D-erythro* C24-SM molecule constructed on the basis of PDB File [26]

kinks of the acyl chain. If the kink is due to a G–T–$\overline{\text{G}}$ conformation (first order kink), the surface area occupied by the sphingosine and acyl chains is estimated to expand by 4.75 Å^2 (=(0.218 Å)^2), which is comparable to approximately 10% increment relative to a surface area 48.9 Å^2 obtained for C24-SM having the trans zig-zag chains by X-ray measurements [8]. For a kink due to a G–T–T–T–$\overline{\text{G}}$ conformation (second order kink), ~30% increment of the surface area could be estimated. Such expansion in the surface area of the acyl chain leads to a conversion into a truncated cone shape of the C24-SM molecule. As a result, it is suggested that the CH_3 end-induced kink conformations for the acyl chain of the C24-SM make it possible for the lipid molecule to adopt the truncated cone packing shape in the inner monolayer of the relatively small size unilamellar vesicle obtained in the present study. In addition, the kink conformations by inserting gauches cause both a shorting of the acyl chain and a widening of the chain-chain distance by which van der Waals interaction energy between the chains is decreased, so that the gel phases are enthalpically higher, thereby giving rise to the smaller main transition enthalpy of the asymmetric chain SMs relative to the C16-SM shown in Table 1. Furthermore, the conversion of the C16-SM MLVs into the small size vesicles induced by the coexisting C22-, and C24-SMs (Fig. 5) indicates an asymmetric distribution of the lipid molecules in the C22-SM/C16-SM and C24-SM/C16-SM mixture systems, thus, the asymmetric chain SMs are obliged to localize in the inner monolayer of bilayer,

resulting in a high surface curvature of the monolayer required for the small size vesicles.

Acknowledgements

This work is supported in part by 'High-Tech Research Center' Project for Private Universities: matching fund subsidy from MEXT (Ministry of Education, Culture, Sports, Science and Technology).

References

1 K. Simons and E. Ikonen, Nature, 387 (1997) 569.
2 A. Rietveld and K. Simons, Biochim. Biophys. Acta, 1376 (1998) 467.
3 A. Prinetti, V. Chigorno, G. Tettamanti and S. Sonnino, J. Biol. Chem., 275 (2000) 11658.
4 U. Ortegren, M. Karlsson, N. Blazic, M. Blomqvist, F. H. Nystrom, J. Gustavsson, P. Fredman and P. Stralfors, Eur. J. Biochem., 271 (2004) 2028.
5 S. H. Untracht and G. G. Shipley, J. Biol. Chem., 252 (1977) 4449.
6 R. Cohen, Y. Barenholz, S. Gatt and A. Dagan, Chem. Physic. Lipids, 35 (1984) 371.
7 T. J. McIntosh, S. A. Simon, D. Needham and C. Huang, Biochemistry, 31 (1992) 2012.
8 P. R. Maulik and G. G. Shipley, Biophys. J., 69 (1995) 1909.
9 L. K. Bar, Y. Barenholz and T. E. Thompson, Biochemistry, 36 (1997) 2507.
10 P. K. Sripada, P. R. Maulik, J. A. Hamilton and G. G. Shipley, J. Lipids Res., 28 (1987) 710.
11 B. Ramstedt and J. P. Slotte, Biophys. J., 76 (1999) 908.
12 A. D. Bangham, M. W. Hill and N. G. A. Miller, Methods Membr. Biol., 1 (1974) 1.
13 G. V. Marinetti, J. Lipid Res., 3 (1962) 1.
14 M. Kodama, T. Miyata and Y. Takaichi, Biochim. Biophys. Acta, 1169 (1993) 90.
15 M. Kodama, H. Aoki and T. Miyata, Biophys. Chem., 79 (1999) 205.
16 M. Kodama and H. Aoki, Surfactant Science Series 93, Thermal Behavior of Dispersed Systems, N. Garti, Ed., Marcel Dekker, New York 2000, p. 247.
17 M. Kodama, H. Hashigami and S. Seki, J. Colloid Interface Sci., 117 (1986) 497.
18 M. Kodama, H. Kato and H. Aoki, Thermochim. Acta, 352-353 (2000) 213.
19 Li, Xin-Min, J. M. Smaby, M. M. Momsen, H. L. Brockman and R. E. Brown, Biophys. J., 78 (2000) 1921.
20 K. S. Bruzik, J. Chem. Soc. Perkin Trans., 1 (1988) 423.
21 Y. Fujino and T. Negishi, Biochim. Biophys. Acta, 152 (1968) 428.
22 B. Ramstedt and J. P. Slotte, Biophys. J., 77 (1999) 1498.
23 Y. Kawasaki, H. Nishikido, A. Kuboki, S. Ohira and M. Kodama, Thermochim. Acta, 431 (2005) 188.
24 L.W. Levin, T. E. Thompson, Y. Barenholz and C. Huang, Biochemistry, 24 (1985) 6282.
25 C. Huang and J. T. Mason, Proc. Natl. Acad. Sci. USA, 75 (1978) 308.
26 Klotho: Biochemical Compounds Declarative Database, http://www.biocheminfo.org/klotho/
27 C. Huang and J. T. Mason, Biochem. Biophys. Acta, 864 (1986) 423.
28 J. T. Mason, C. Huang and R. L. Biltonen, Biochemistry, 20 (1981) 6086.

DOI: 10.1007/s10973-007-8968-9